

# Dynamic Modelling of a Solar Energy System with Vehicle to Home and Vehicle to Grid Option for Newfoundland Conditions

Raghul Suraj Sundararajan, M. Tariq Iqbal

**Abstract** — The dynamic modelling of a solar energy system with vehicle to home (V2H) and vehicle to grid (V2G) options for Newfoundland conditions is discussed in this paper. A site (13 Polina Road) was chosen in St. John's, Newfoundland, Canada. An optimized system was built for the chosen site using BEopt, Homer, and MATLAB software's to meet the house's energy demand. Furthermore, smart current sensors installed in the house are used to incorporate the V2H and V2G concepts. The Nissan Leaf's battery is used to supply household loads in V2H operation mode when the power supplied by the PV panel and the storage energy in the inhouse battery is less than the load's energy demand. In V2G mode, the vehicle is only linked to grid. Along with the simulation results, detailed system dynamic modelling is also presented. There are nine different system control modes that are proposed and simulated.

**Index Terms** — PV, V2H, V2G, Renewable energy, Hybrid power systems.

## I. INTRODUCTION

Electric vehicles (EVs) are the next wave in the global transportation industry. EV's have various advantages, more powerful, emit no pollution and act as mobile power reservoirs. EV's need to be charged, renewable sources of energy, such as solar energy systems, help satisfy the energy demand and also to reduce the carbon footprint [1] Since renewables are inherently variable, backup battery is required. Since EVs act as reservoirs, the concept of Vehicle to Home (V2H) and Vehicle to Grid (V2G) can be implemented [2], [3]. The proposed system implements V2H and V2G concept. The in-house battery acts as backup battery, to supply uninterrupted power the home load's when the power produced by PV is not sufficient to meet the load's energy demand. The Nissan Leaf (40kW variant) is being considered as EV, for use in the V2H concept. Furthermore, the implemented system has level 1 and level 2 chargers for charging the Nissan Leaf's battery during charging mode, as well as a converter for charging the inhouse battery and powering the load at the same time. Until the produced power is less than the load's energy requirement, the designed system uses PV as the primary source of power. However, if the power produced by PV was less compared to load's energy demand, the inhouse battery is used to power the loads in this situation. When the system reaches 30% SOC, it switches to V2H, which means the Nissan Leaf's battery will be discharged to satisfy the load's energy demand [4]. In V2G

mode, the car disconnects from the house and feeds power to the grid [5], [6]

In this paper, we present a solution that addresses this problem by combining the Vehicle to Home (V2H) and Vehicle to Grid (V2G) principles, as well as a hybrid PV system [7]. For system sizing and dynamic modelling, BEopt, HOMER, and MATLAB were used.

## II. SITE DETAILS

### A. Selected Site and Solar Insolation

The research location was selected as 13 Polina Road in St. John's, Newfoundland, Canada. It has a total area of 185.89 m<sup>2</sup>. In St. John's, Newfoundland, Canada, Fig. 1 depicts a monthly solar radiation and clearness index profile for the chosen region. The clearness index varies from 0.20 to 0.30. The average solar insolation is 3.15 kWh/m<sup>2</sup>/day, with a range of 1.28 kWh/m<sup>2</sup>/day to 5.14 kWh/m<sup>2</sup>/day.

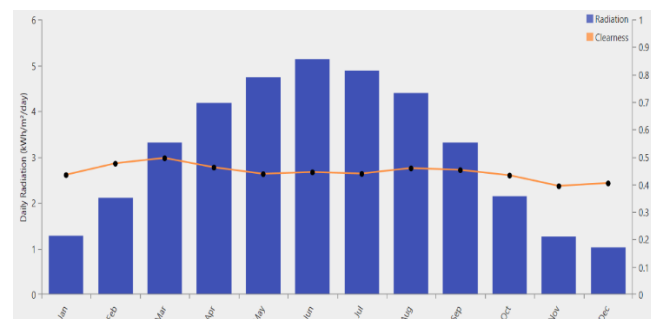


Fig. 1. Solar insolation and clearness index of selected site.

### B. Sites Power Requirement from BEopt

The annual power demand for the chosen site was calculated using BE opt tools. The annual power consumption of the house is approximately 21111 kWh. This covers all loads in the building, such as heaters, boilers, lighting, ventilation, and other factors including plugin loads.

### C. Sites Load and Photovoltaic Panel Area Calculation

The daily load requirement for the site is 11.90 kW. The hourly electricity demand rises at 6 a.m. and falls by 9 p.m., with an all-time high between 6 and 7 PM. Fig. 2 shows the seasonal load profile from HOMER, which shows that the months of November to April have higher per hour energy demand than the months of May to October.

Submitted on May 23, 2021.

Published on June 13, 2021.

Raghul Suraj Sundararajan, Memorial University of Newfoundland, Canada.  
(e-mail: rssundararaj@mun.ca)

M. Tariq Iqbal, Memorial University of Newfoundland, Canada.  
(e-mail: tariq@mun.ca)

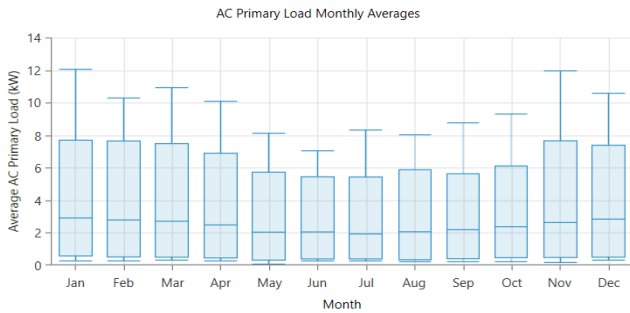


Fig. 2. Annual load chart from HOMER.

### III. SYSTEM SIMULATION

The software Hybrid Optimization of Multiple Energy Resources (HOMER) was used to size the system. A schematic of the proposed system is shown in Fig. 4. The solar panel used was a Canadian Solar CS6U-340M, the battery was a Trojan SAGM 12 105, the inverter was 20 kW, the home load profile was 57.8 kWh/d with a peak of 11.90 kW and a backup, a 10 kW genset is installed, which has no effect on the system's dynamics.

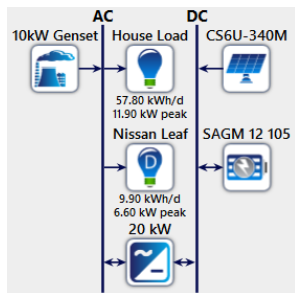


Fig. 4. Schematic of proposed system in HOMER.

#### A. Photovoltaic Panel

The Canadian Solar CS6U 340M module, with a 340 W output and a 1.8 m<sup>2</sup> surface area, was used in this design.

In St. John's, the average daily sunlight is 1633 hours for 272 days.

$$\text{Output from BEopt} = 21111 \text{ kWh/year}$$

$$\text{Per day} = 57.8 \text{ kWh/day}$$

$$\text{Power Output} = \frac{\text{Energy usage per day}}{\text{Number of full sun hours per day}}$$

$$\text{Power Output} = 12.930 \text{ kW}$$

For PV sizing considering derating factor as 0.8

$$= \frac{\text{Power output}}{\text{derating}}$$

$$= 16.1633 \text{ kW}$$

$$\text{PV size array} = \frac{\text{Total calculated capacity of PV}}{340W}$$

For calculated power output

$$= 38 \text{ Modules}$$

For derating factor

$$= 48 \text{ Modules}$$

Area calculation

Area of one Canadian solar CS6U 340 M module is 1.88m<sup>2</sup>

For desired power output

$$= 38 \times 1.88$$

$$= 71.44 \text{ m}^2$$

For derating factor

$$= 48 \times 1.88$$

$$= 90.24 \text{ m}^2$$

$$\text{Available area} = 185.89 \text{ m}^2$$

Bus voltage = 48 V

For desired power output, number of strings = 20 Strings

Number of panels in each string = 2

Including derating factor the number of strings = 24 Strings

#### B. Battery

For this application, the Trojan SAGM 12 105 battery was selected. The following is the battery calculation, including three days of backup. The calculations show that 360 batteries are needed without backup. Since the design included a 10kW backup generator, the number of batteries needed was reduced to 80.

$$\frac{Wh}{\text{day}} = 57804 \frac{Wh}{\text{day}}$$

$$3 \text{ days} = 57804 \times 3 = 173413 \text{ Wh}$$

$$40\% \text{ DOD} = \frac{173413}{0.4} = 433532.5 \text{ Wh}$$

$$\text{Temp Cons} (> 80F) = 433532.5 \times 1 = 433532.5 \text{ Wh}$$

$$\text{Ah cap of Bt bank} = \frac{433532.5}{48} = 9031.92 \text{ Ah}$$

$$\text{Number of Batteries} = \left( \frac{9031.92}{100} \right) \times 4 = 360 \text{ Nos}$$

#### C. Nissan Leaf – 40 kW variant

Nissan Leaf with a 40 kWh lithium-ion battery pack and a 6.6 kW onboard charger is considered in this concept. A built-in bidirectional converter for charging and discharging is another benefit of the Nissan Leaf (reeling power to home). Charging and discharging are the two modes of operation for the Nissan Leaf. Nissan Leaf is reeling out power or discharging its battery, when the PV panels and battery are unlikely to fulfill the energy demand of the home load, this mode is used [8], [9]. When the Nissan Leaf is in charging mode, the following is assumed. The electric vehicle is charged with the excess energy generated or stored after the home loads are met [10].

#### D. Inverter

The peak load value is about 19.90 kW and deferrable loads peak value is 6.60kW, an inverter with a 20 kW output capacity is considered for the design. In this case, the inverter has two outputs: 120 V and 240 V.

### IV. DYNAMIC MODELLING

Simulink was used to simulate the proposed architecture. PV array, MPPT controller, in-house battery, boost converters, inverter, level 1 and level 2 chargers, Nissan Leaf battery and V2G inverter are all included in the simulation. The overall block diagram of the proposed system is shown in Fig. 5. PV power is used to charge the in-house battery via a charger, and an inverter with two outputs at 120 V and 240 V is used to convert the stored power in the battery to AC to power the house load. Furthermore, a Nissan leaf charger with level 1 and level 2 charging capabilities [8] is designed, as well as a converter to step down 360 V to 48 V, which is used to charge the in-house battery and simultaneously powering the house loads [9] and a 10 kW genset is incorporated which is used only as a backup and has no impact on dynamics of the system. Overview of simulated system is illustrated in Fig. 6. The system is simulated for

charging and discharging the in-house battery, powering loads with the in-house battery, a dual outlet inverter that outputs 120 V and 240 V, a Nissan leaf charger with level 1 and level 2 charging.

Discharge Nissan Leaf to charge inhouse battery, discharge inhouse battery at night to charge Nissan Leaf, discharge Nissan Leaf to implement V2G mode and a dump load to remove excess power. Automatic state of charge overrides is included in the system, with 30 percent SOC charge ON (inhouse battery) and 40 percent SOC charge ON (Nissan Leaf battery) for the inhouse battery and Nissan Leaf, respectively. Fig. 6 shows the full Simulink simulation block diagram.

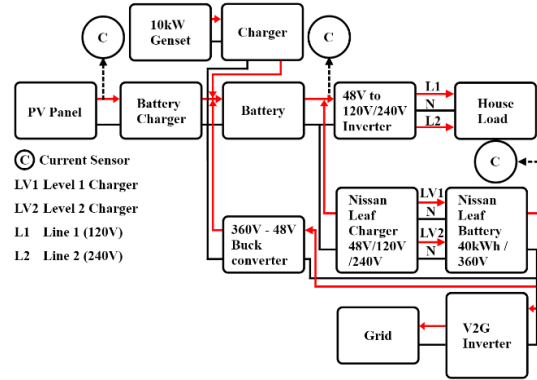


Fig. 5. Overall block diagram.

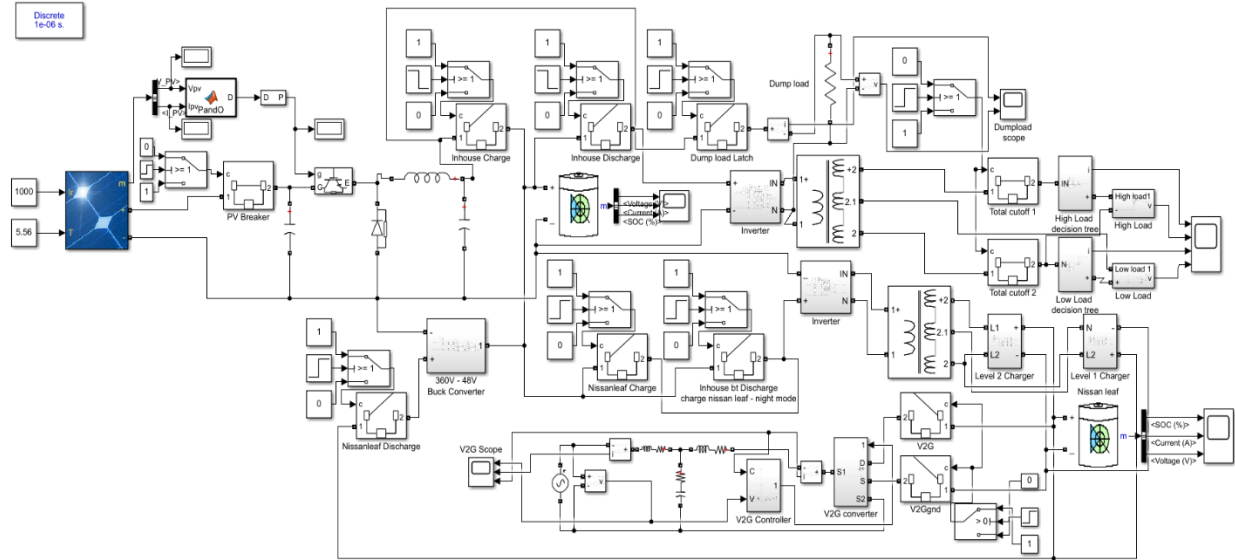


Fig. 6. Overview of simulated system in Simulink.

### A. MPPT Algorithm

Maximum power point tracking (MPPT) is a concept that entails adjusting PV impedance in response to changing irradiance in order to get the most power out of a PV panel. In this simulation, the MPPT controller employs the Perturbation and Observation (P&O) algorithm. In the P&O algorithm, the voltage is continuously perturbed, and the inverter duty cycle is updated based on the output observation. This algorithm is the best at monitoring the maximum point even though there is a large drop or spike in irradiance.

Furthermore, the simulation was carried out incorporating eight modes representing different modes [10] of operation. Fig. 7 illustrates the implemented switching control logic.

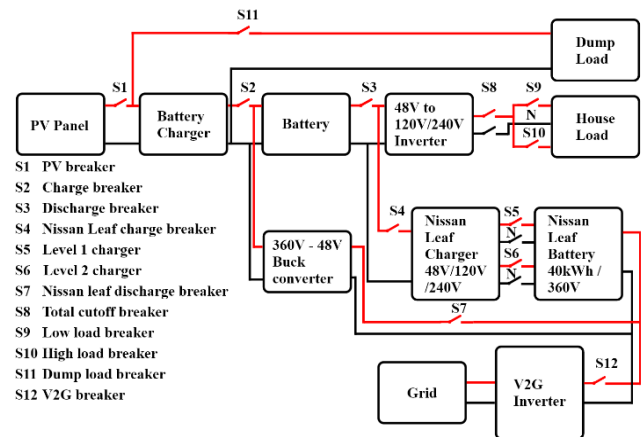


Fig. 7. Switching control logic system.

TABLE I: SWITCH CONTROL SCHEME FOR THE PROPOSED SYSTEM

Modes	S1	S2	S3	S4	S5	S6	S7	S8	S9	S10	S11	S12
Mode 1	ON	ON	ON	OFF	OFF	OFF	OFF	ON	ON	OFF	OFF	OFF
Mode 2	OFF	OFF	ON	OFF	OFF	OFF	OFF	ON	OFF	ON	OFF	OFF
Mode 3 (Level 1)	ON	ON	ON	ON	ON	OFF	OFF	ON	ON	OFF	OFF	OFF
Mode 3 (Level 2)	ON	ON	ON	ON	OFF	ON	OFF	ON	ON	OFF	OFF	OFF
Mode 4	OFF	OFF	OFF	OFF	OFF	OFF	ON	ON	OFF	ON	OFF	OFF
Mode 5	-	ON	ON	-	-	-	-	-	-	-	-	OFF
Mode 6	OFF	ON	OFF	OFF	OFF	OFF	OFF	OFF	-	-	OFF	OFF
Mode 7	ON	OFF	OFF	OFF	OFF	OFF	OFF	OFF	OFF	OFF	ON	OFF
Mode 8 (Level 1)	OFF	OFF	ON	ON	ON	OFF	OFF	ON	ON	OFF	OFF	OFF
Mode 8 (Level 2)	OFF	OFF	ON	ON	OFF	ON	OFF	ON	ON	OFF	OFF	OFF
Mode 9	OFF	OFF	OFF	OFF	OFF	OFF	OFF	OFF	OFF	OFF	OFF	ON

### B. Model 1 – Inhouse Battery Charge Mode

The PV output is used to charge the in-house battery and power the loads in this mode. The energy consumption of the loads is minimal in this situation. The extra energy is put to good use by charging the battery. The control logic for charging inhouse battery is depicted in Fig. 9. Switches S1, S2, S3, S8, S9 are switched ON to implement mode 1 as seen in Fig. 8 and Table I. The current and voltage graphs for the low load are seen in Fig. 9 and 10. The voltage and current of the load are 120V and 12A, respectively.

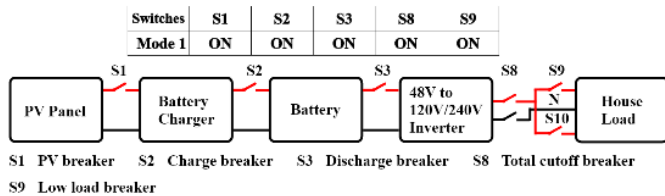


Fig. 8. Control logic for in-house battery charging.

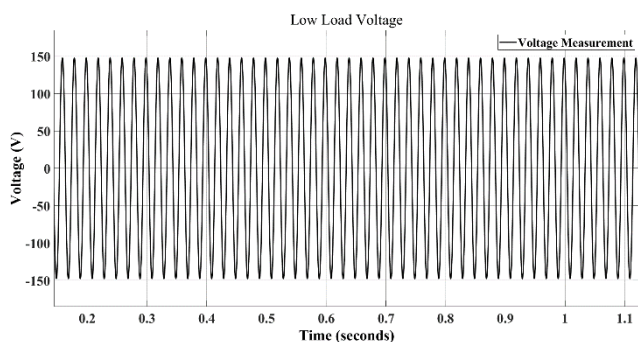


Fig. 9. Low load voltage output graph.

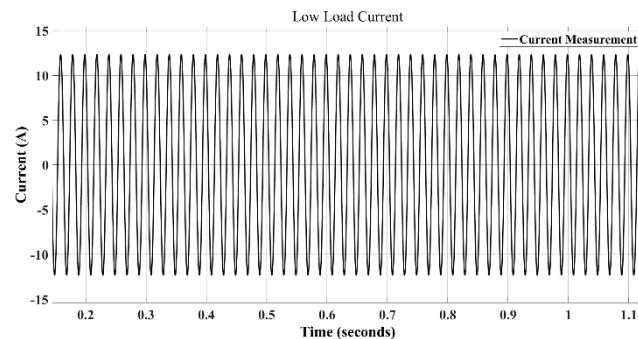


Fig. 10. Low load current output graph.

### C. Mode 2 – Inhouse Battery Discharge Mode

PV output is low in this mode relative to the load's energy requirement. The load is powered by the in-house battery in this situation. The control logic for in-house battery in discharge mode is seen in Fig. 11. A two-output inverter is also used, with output voltages of 120 V and 240 V. Switches S3, S8, S10 are turned ON to implement mode 2 as seen in Fig. 10 and Table I. The current and voltage graphs for high loads are seen in Fig. 12 and 13. In this case, the load is 240 V and 27 A.

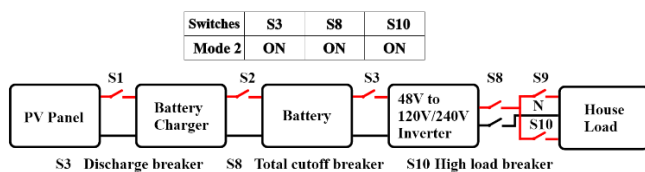


Fig. 11. Control logic for Inhouse battery discharge.

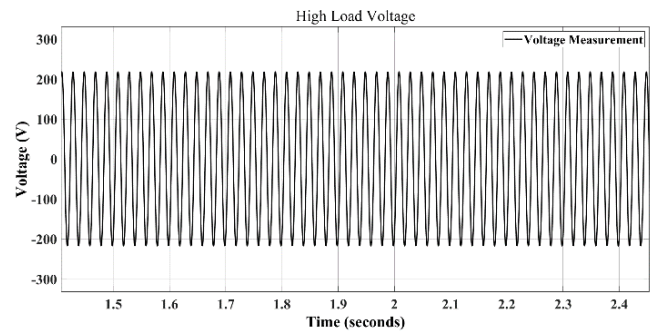


Fig. 12. High load voltage output graph.

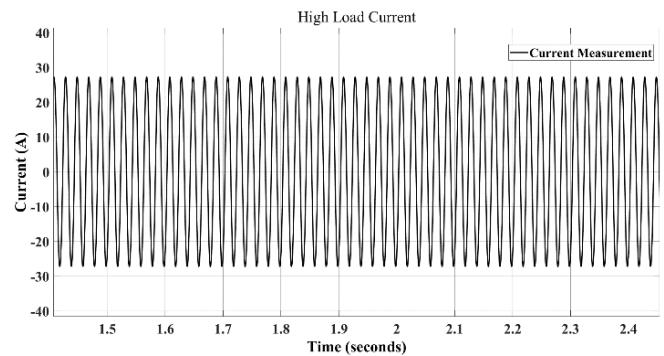


Fig. 13. High load current output graph.

### D. Mode 3 – Nissan Leaf Charge Mode

When the PV output exceeds the load's energy demand and the in-house batteries' SOC exceeds 60%, the device will charge the Nissan Leaf battery [11]. Level 1 (120 V, 14 A) and level 2 (240 V, 20 A) charging are both used in the charger. The control logic for Nissan Leaf at level 1 and level 2 charging modes are depicted in Fig. 14 and 15, respectively. The power for the level 1 and level 2 chargers is supplied by an inverter. Furthermore, boost converters have been integrated into the chargers to increase the voltage to 360 V, which is the charging voltage of the Nissan Leaf battery. Switches S1, S2, S3, S4, S5, S8, S9 are turned ON to implement mode 3 (level 1 charging) as seen in Fig. 14 and Table I. For mode 3 (level 2 charging) switches S1, S2, S3, S4, S6, S8, S9 are turned ON and switches S5, S10, S11 are turned OFF as seen in Fig. 15 and Table I. The charging current graphs for level 1 and level 2 charging are seen in Fig. 17 and 18. Fig. 19 depicts the state of charge (SOC) of a Nissan Leaf battery. The developed system includes both level 1 and level 2 charging, with the output from level 2 charging is visible between 5 and 10 seconds and the output from level 1 charging is visible between 10 and 15 seconds [12], [13].

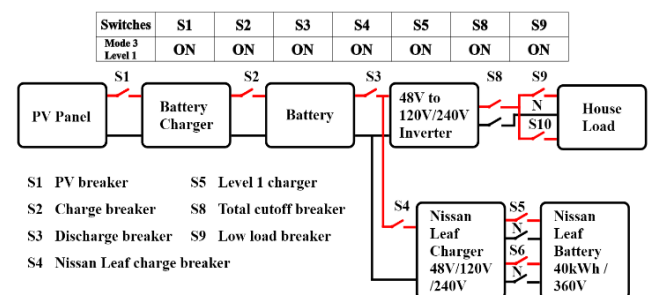


Fig. 14. Control logic for Nissan Leaf at level 1 charging mode.

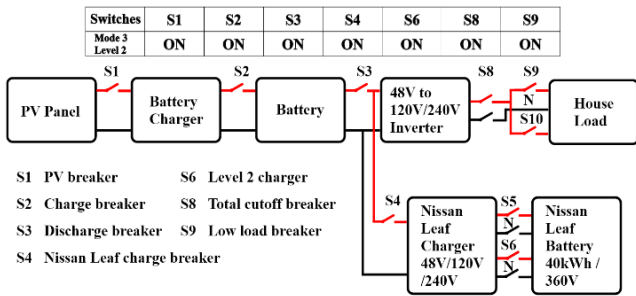


Fig. 15. Control logic for Nissan Leaf at level 2 charging mode.

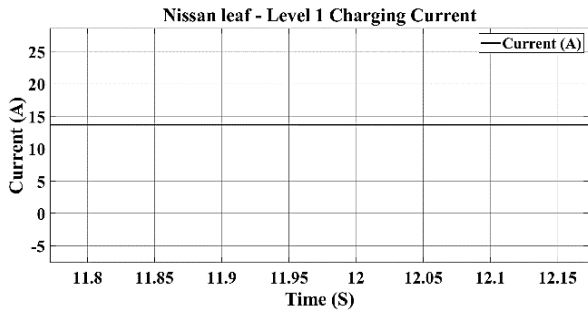


Fig. 16. Level 1 charging current output graph.

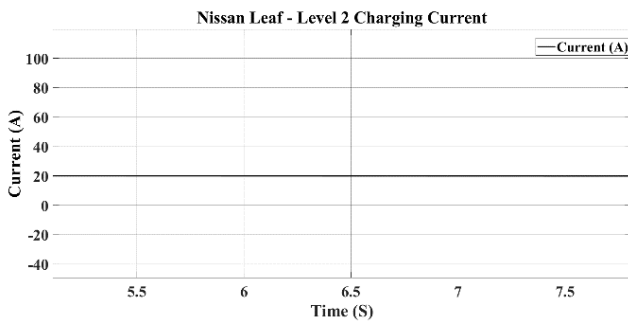


Fig. 17. Level 2 charging current output graph.

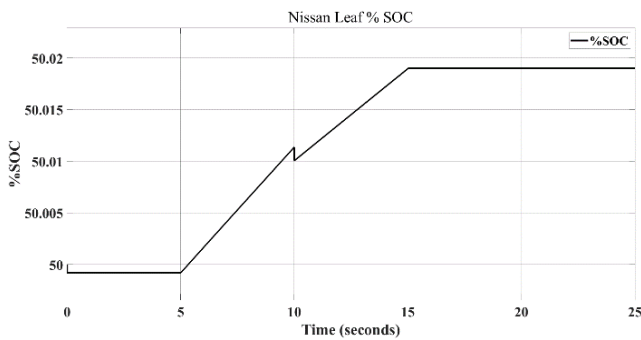


Fig. 18. Nissan Leaf's SOC graph.

#### E. Mode 4 – Nissan Leaf Discharge Mode

When the PV output is less than the load energy demand and the inhouse batterie SOC is less than 30%, Nissan Leaf reels out the stored energy to the house to satisfy the load energy demand [14], [15]. The control logic for Nissan Leaf in discharge mode is depicted in Fig. 18. To charge the battery and power the load at the same time, a buck converter is used to reduce the high voltage (360 V) from the Nissan Leaf's battery to 48 V [16]. Switches S7, S8, S10 are turned ON to implement mode 4 as seen in Fig. 18 and Table I. The SOC graph for the Nissan Leaf as shown in Fig. 19. Because of Nissan Leaf's discharge mode execution, the inhouse battery was on a discharge loop between the time intervals of 5

seconds and 15 seconds in Fig. 19, and then it began to charge.

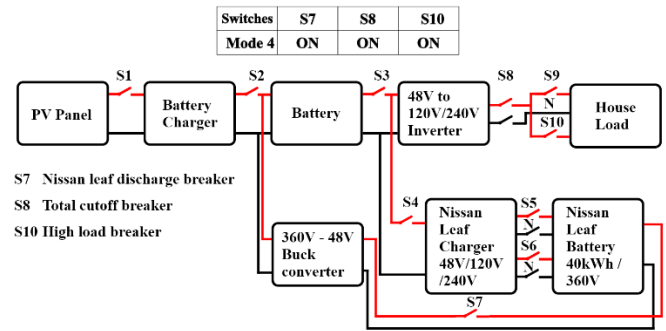


Fig. 19. Control logic for Nissan Leaf in discharge mode.

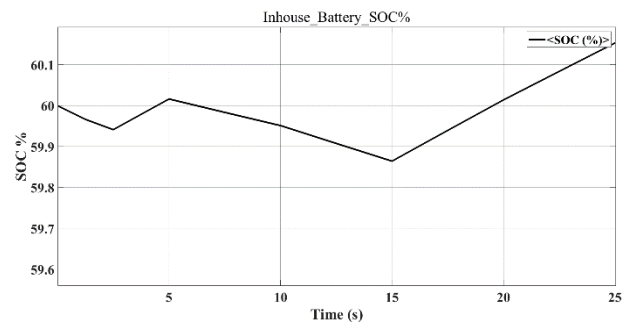


Fig. 20. Inhouse batterie's SOC graph.

#### F. Mode 5 – Inhouse Battery Protection Mode

This mode is included to assist in the saving of the in-house battery by tracking the battery's SOC. When the SOC of in-house batteries drop below 30%, the 30% SOC breaker and the 30% SOC charge on breaker will all go HIGH to charge the battery. Switches S2, S3 are switched ON to implement mode 5 as seen in Table I.

#### G. Mode 6 – System Isolation Mode

The total cutoff breaker is switched on in this mode because the PV output is less than the loads energy demand, the inhouse batteries SOC is less than 30%, and the Nissan leaf SOC is less than 40%. This is designed to separate the system from the load and prevent it from failing. Switch S2 is switched ON to implement mode 6 as seen in Table I.

#### H. Mode 7 – Excess Power Management Mode

When the power produced by PV exceeds the energy demand of the load, the in-house battery and Nissan Leaf's battery are charged, and a dump load is used to dissipate the excess power. The control logic for excess power mode is illustrated in Fig. 20. Switches S1 and S11 are switched ON to implement mode 7 as seen in Fig. 20 and Table I.

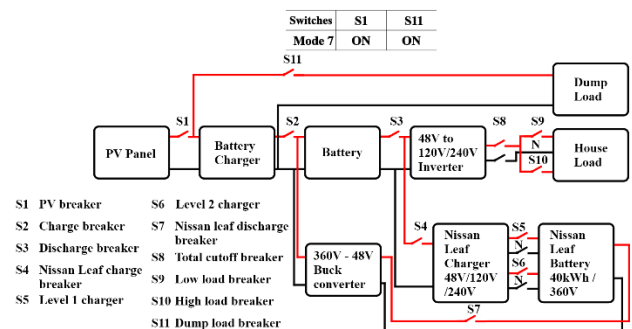


Fig. 21. Control logic for excess power mode.

### I. Mode 8 – Nighttime Charging Mode

The power stored in the inhouse battery is used to charge the Nissan Leaf's battery at night while the loads energy demand is much lower and the inhouse battery's SOC is greater than 60% [17]. The control logic for nighttime level 1 and level 2 charging mode is depicted in Fig. 21 and Fig. 22. Switches S3, S4, S5, S8, S9 are switched ON to implement mode 8 at level 1 charging as seen in Fig. 21 and Table 1. In mode 8 level 2 charging switches S3, S4, S6, S8, S9 are switched ON as seen in Fig. 22 and Table I.

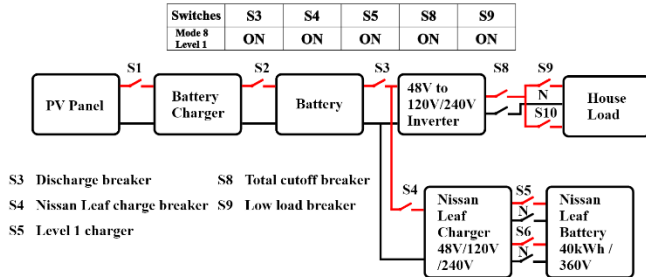


Fig. 22. Control logic for nighttime level 1 charging mode.

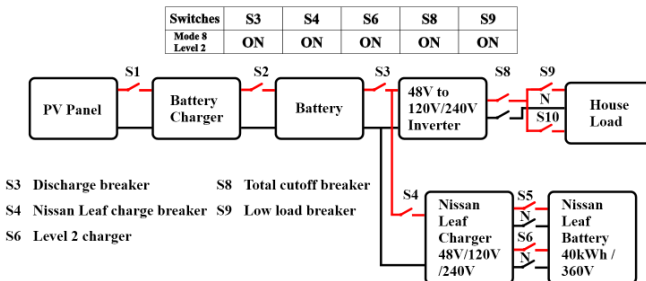


Fig. 23. Control logic for nighttime level 2 charging mode.

### J. Mode 9 – V2G Mode

In this mode the vehicle isolates itself from home and reels power to the grid [18], [19]. Fig. 23 illustrates the control logic for vehicle to grid (V2G) mode and Fig. 24 illustrates the vehicle to grid mode design in MATLAB. Switch S12 is switched ON to implement mode 9 as seen in Fig. 23 and Table I. The implemented design comprises of PLL block, Current controller (PI) and PWM generator [20]. Fig. 25 illustrates the implemented PI and PLL controller design. PLL is used to generate a reference signal and the signal is in phase with the actual voltage. The reference signal is used for implementation of current controller in a grid connected inverter. Further the Vgrid voltage is fed to a lowpass filter as shown in equation 1 and Fig. 25. Substituting equation 2 in equation 1 gives the transfer function in equation 3. The magnitude and phase of lowpass filter can be in equation 4. Assuming equation 5,  $\omega_c$  is replaced by  $\omega$  in equation 6. Further simplification results in equation 7. Adding a second low pass filter as seen in equation 8, the magnitude becomes  $1/2$  and the angle would be  $-90$  as seen in equation 9. Finally, multiply the output from second low pass filter with 2 to get an output signal (alpha) that is same as input with 90-degree phase shift as seen in Fig. 25.

$$TF = \frac{\omega_c}{s + \omega_c} \quad (1)$$

where,  $\omega_c$  = corner frequency.

$$s = j\omega \quad (2)$$

$$TF = \frac{\omega_c}{j\omega + \omega_c} \quad (3)$$

$$TF = \frac{\omega_c}{\sqrt{\omega^2 + \omega_c^2}} < \tan^{-1}\left(\frac{\omega}{\omega_c}\right) \quad (4)$$

$$\omega = \omega_c \quad (5)$$

$$TF = \frac{\omega}{\sqrt{\omega^2 + \omega^2}} < \tan^{-1}\left(\frac{\omega}{\omega}\right) \quad (6)$$

$$TF = \frac{1}{\sqrt{2}} < -45 \quad (7)$$

$$TF = \frac{1}{\sqrt{2}} \times \frac{1}{\sqrt{2}} < -45 - 45 \quad (8)$$

$$TF = \frac{1}{2} < -90 \quad (9)$$

Further to implement PLL, Vgrid and alpha signals are converted into DQ signals. A control system is set for Q output, the error between Q and Q ref is set as zero and is fed to a PI controller. The output from PI controller gives the angle information which is integrated to get  $\omega t$ . Output from the Integrator is fed to alpha beta to DQ transformation block. In this case the output from PI controller is aligned with input signal. Hence this value can be used to generate active and reactive current reference signal as seen in Fig. 25 [21], [22].

The generated reference signal is added with grid voltage which generates the reference signal for generation of PWM. A unipolar generation scheme is implemented in the designed system. The reference voltage is compared with the triangular carrier wave and positive and negative references are compared. Output from each comparator is inverted and connected to the gate terminal of each IGBT as seen in Fig. 25. Fig. 26, 27, 28 illustrates the grid's voltage graph, grid's current graph and inverter current graph, respectively.

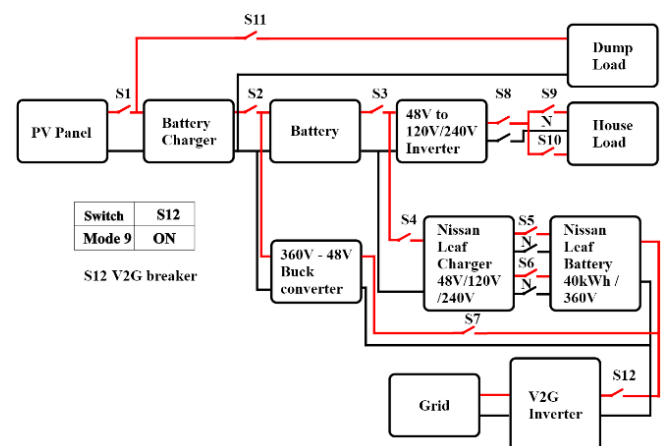


Fig. 24. Control logic for vehicle to grid (V2G) mode.

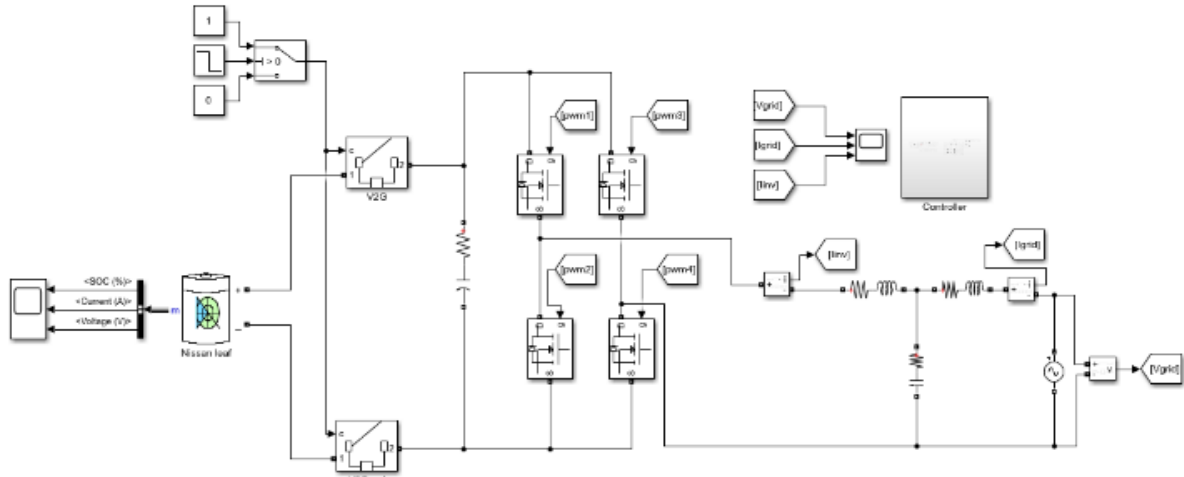


Fig. 25. Vehicle to Grid (V2G) mode design in MATLAB.

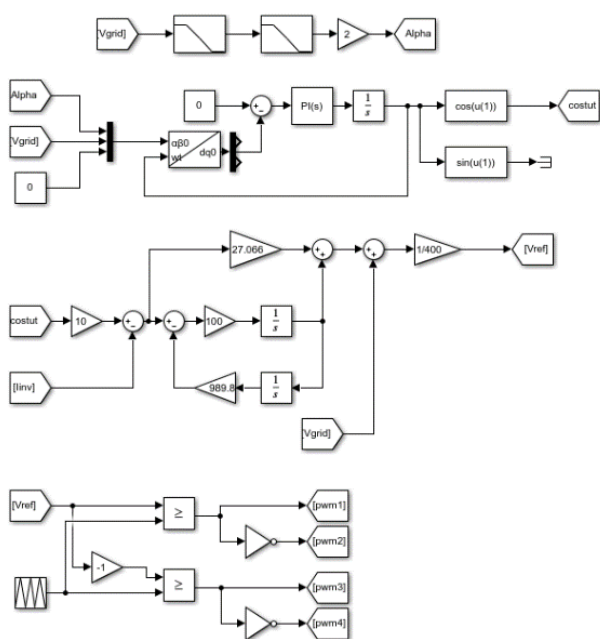


Fig. 26. V2G controller – PLL, PI controller.

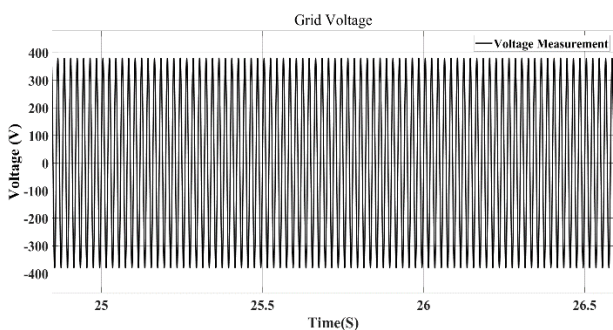


Fig. 27. Grid voltage graph – V2G mode.

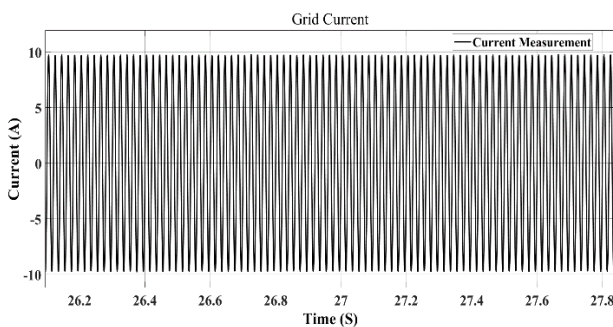


Fig. 28. Grid current graph – V2G mode.

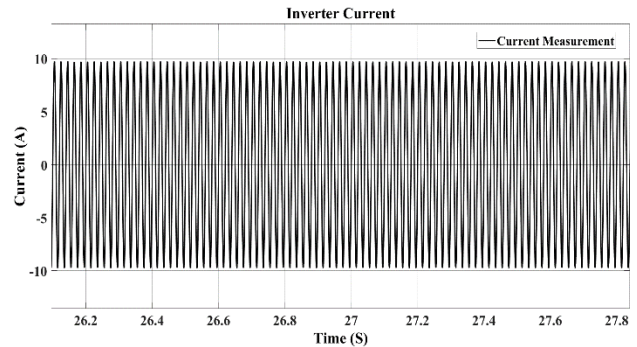


Fig. 29. Inverter current graph – V2G mode.

## V. CONCLUSION

For Newfoundland conditions, dynamic modelling of a solar energy system with vehicle to home and vehicle to grid options was successfully designed and simulated. The solar insolation for Newfoundland is 3.15 kWh/m<sup>2</sup>/day, as seen in Fig. 1. The PV panels used are 340W modules that generate 16.3984 kW and are configured in 24 strings, each with two panels. Nissan Leaf is configured as a deferrable load of 9.90 kWh/d and 6.60 kW peak, a 12.5 kW commercially available inverter, 80 Trojan SAGM 12 105 batteries, each rated at 12 V and 100 Ah, a backup genset of 10 kW, and a vehicle to grid (V2G) inverter as seen in Fig. 7. In the simulation that has been implemented, there are nine main operating modes: i) inhouse battery charging mode – PV power is used to charge the inhouse battery while simultaneously powering the loads; ii) inhouse battery discharge mode – The stored power in the inhouse house battery is used to meet the loads energy demand; iii) Nissan Leaf charging mode – The available power is used to charge the Nissan Leaf after satisfying the load's energy demand and charging the in-house battery; iv) Nissan Leaf discharge mode: the loads have a high energy demand, but the PV and in-house battery SOC is low [23]. Nissan Leaf draws on its accumulated energy to meet the load's energy demand [24]; v) in-house battery protection mode – avoids degenerative discharge of the in-house battery; vi) system isolation mode – prevents system failure; vii) excess power management mode – manages excess power generated; viii) nighttime charging mode – charges Nissan Leaf overnight in preparation for use the next day; ix) V2G mode – power is reeled to the grid. The system is scalable: it can be extended

to include parking lots [25], several houses can be joined to form a microgrid [26], and it can control or assist the grid (V2G) [27]. The V2X model, in which vehicles are used to schedule loads [28], power multiple homes, businesses, or an entire city, and transfer power from one vehicle to another [29], will be studied further. [30]-[33].

#### ACKNOWLEDGMENT

The authors acknowledge LUX Flavors PVT Ltd for funding the research.

#### REFERENCES

- [1] R. Hemmati, H. Mehrjerdi, N. A. Al-Emadi and E. Rakhshani, "Mutual Vehicle-to-Home and Vehicle-to-Grid Operation Considering Solar-Load Uncertainty," 2019 2nd International Conference on Smart Grid and Renewable Energy (SGRE), 2019, pp. 1-4, doi: 10.1109/SGRE46976.2019.9020685.
- [2] F. M. Shakeel and O. P. Malik, "Vehicle-To-Grid Technology in a Micro-grid Using DC Fast Charging Architecture," 2019 IEEE Canadian Conference of Electrical and Computer Engineering (CCECE), 2019, pp. 1-4, doi: 10.1109/CCECE.2019.8861592.
- [3] N. Z. Xu and C. Y. Chung, "Reliability Evaluation of Distribution Systems Including Vehicle-to-Home and Vehicle-to-Grid," in IEEE Transactions on Power Systems, vol. 31, no. 1, pp. 759-768, Jan. 2016, doi: 10.1109/TPWRS.2015.2396524.
- [4] S. Rezaee, E. Farjah and B. Khorramdel, "Probabilistic Analysis of Plug-In Electric Vehicles Impact on Electrical Grid Through Homes and Parking Lots," in IEEE Transactions on Sustainable Energy, vol. 4, no. 4, pp. 1024-1033, Oct. 2013, doi: 10.1109/TSTE.2013.2264498.S.
- [5] I. Sami Z. Ullah, K. Salman, I. Hussain, S.N. Ali, B. Khan, et al, "A Bidirectional Interactive Electric Vehicles Operation Modes: Vehicle-to-Grid (V2G) and Grid-to-Vehicle (G2V) Variations Within Smart Grid," 2019 International Conference on Engineering and Emerging Technologies (ICEET), 2019, pp. 1-6, doi: 10.1109/CEET1.2019.8711822.N.
- [6] H. Turker and I. Colak, "Multiobjective optimization of Grid-Photovoltaic- Electric Vehicle Hybrid system in Smart Building with Vehicle-to-Grid (V2G) concept," 2018 7th International Conference on Renewable Energy Research and Applications (ICRERA), 2018, pp. 1477-1482, doi: 10.1109/ICRERA.2018.8567002.
- [7] C. Liu, K. T. Chau, D. Wu and S. Gao, "Opportunities and Challenges of Vehicle-to-Home, Vehicle-to-Vehicle, and Vehicle-to-Grid Technologies," in Proceedings of the IEEE, vol. 101, no. 11, pp. 2409-2427, Nov. 2013, doi: 10.1109/JPROC.2013.2271951.
- [8] Y. Wi, J. Lee and S. Joo, "Electric vehicle charging method for smart homes/buildings with a photovoltaic system," in IEEE Transactions on Consumer Electronics, vol. 59, no. 2, pp. 323-328, May 2013, doi: 10.1109/TCE.2013.6531113.Y.
- [9] B. Kim, "Smart charging architecture for between a plug-in electrical vehicle (PEV) and a smart home," 2013 International Conference on Connected Vehicles and Expo (ICCVE), 2013, pp. 306-307, doi: 10.1109/ICCVE.2013.6799811.V.
- [10] V. Monteiro, J. G. Pinto and J. L. Afonso, "Operation Modes for the Electric Vehicle in Smart Grids and Smart Homes: Present and Proposed Modes," in IEEE Transactions on Vehicular Technology, vol. 65, no. 3, pp. 1007-1020, March 2016, doi: 10.1109/TVT.2015.2481005.X.
- [11] V. Monteiro, T. J. C. Sousa, C. Couto, J. S. Martins, A. A. N. Melendez and J. L. Afonso, "A Novel Multi-Objective Off-Board EV Charging Station for Smart Homes," IECON 2018 - 44th Annual Conference of the IEEE Industrial Electronics Society, 2018, pp. 1983-1988, doi: 10.1109/IECON.2018.8591325.
- [12] A. Ito, A. Kawashima, T. Suzuki, S. Inagaki, T. Yamaguchi and Z. Zhou, "Model Predictive Charging Control of In-Vehicle Batteries for Home Energy Management Based on Vehicle State Prediction," in IEEE Transactions on Control Systems Technology, vol. 26, no. 1, pp. 51-64, Jan. 2018, doi: 10.1109/TCST.2017.2664727.V.
- [13] J. G. Pinto et al., "Bidirectional battery charger with Grid-to-Vehicle, Vehicle-to-Grid and Vehicle-to-Home technologies," IECON 2013 - 39th Annual Conference of the IEEE Industrial Electronics Society, 2013, pp. 5934-5939, doi: 10.1109/IECON.2013.6700108.
- [14] J. Gupta and B. Singh, "A Bidirectional Home Charging Solution for an Electric Vehicle," 2019 IEEE International Conference on Environment and Electrical Engineering and 2019 IEEE Industrial and Commercial Power Systems Europe (EEEIC / I&CPS Europe), 2019, pp. 1-6, doi: 10.1109/EEEIC.2019.8783612.
- [15] V. Monteiro, B. Exposto, J. C. Ferreira and J. L. Afonso, "Improved Vehicle-to-Home (iV2H) Operation Mode: Experimental Analysis of the Electric Vehicle as Off-Line UPS," in IEEE Transactions on Smart Grid, vol. 8, no. 6, pp. 2702-2711, Nov. 2017, doi: 10.1109/TSG.2016.2535337.
- [16] Y. Wang, O. Sheikh, B. Hu, C. Chu and R. Gadh, "Integration of V2H/V2G hybrid system for demand response in distribution network," 2014 IEEE International Conference on Smart Grid Communications (SmartGridComm), 2014, pp. 812-817, doi: 10.1109/SmartGridComm.2014.7007748.
- [17] H. Turker, "Optimal Charging of Plug-in Electric Vehicle (PEV) in Residential Area," 2018 IEEE Transportation Electrification Conference and Expo (ITEC), 2018, pp. 243-247, doi: 10.1109/ITEC.2018.8450125.
- [18] H. Chtioui and G. Boukettaya, "Vehicle-to-Grid Management Strategy for Smart Grid Power Regulation," 2020 6th IEEE International Energy Conference (ENERGYCon), 2020, pp. 988-993, doi: 10.1109/ENERGYCon48941.2020.9236530.M.
- [19] D. -C. Urcan and D. Bicã, "Integrating and modeling the Vehicle to Grid concept in Micro-Grids," 2019 International Conference on ENERGY and ENVIRONMENT (CIEM), 2019, pp. 299-303, doi: 10.1109/CIEM46456.2019.8937610.
- [20] A. K. Verma, B. Singh and D. T. Shahani, "Grid to vehicle and vehicle to grid energy transfer using single-phase bidirectional AC-DC converter and bidirectional DC-DC converter," 2011 International Conference on Energy, Automation and Signal, 2011, pp. 1-5, doi: 10.1109/ICEAS.2011.6147084.
- [21] Wooyoung Choi, Woongkul Lee, Di Han and B. Sarlioglu, "Shunt-Series-Switched Multi-Functional Grid-Connected Inverter for Voltage Regulation in Vehicle-to-Grid Application," 2018 IEEE Transportation Electrification Conference and Expo (ITEC), 2018, pp. 961-965, doi: 10.1109/ITEC.2018.8450249.
- [22] B. Rajalakshmi, U. Soumya and A. G. Kumar, "Vehicle to grid bidirectional energy transfer: Grid synchronization using Hysteresis Current Control," 2017 International Conference on Circuit, Power and Computing Technologies (ICCPCT), 2017, pp. 1-6, doi: 10.1109/ICCPCT.2017.8074244.
- [23] L. S. de Souza Pelegrino, M. L. Heldwein and G. Waltrich, "Low-intrusion vehicle-to-home concept," 2016 International Conference on Electrical Systems for Aircraft, Railway, Ship Propulsion and Road Vehicles & International Transportation Electrification Conference (ESARS-ITEC), 2016, pp. 1-6, doi: 10.1109/ESARS-ITEC.2016.7841410.
- [24] M. S. Shemami, S. M. Amrr, M. S. Alam and M. S. Jamil Asghar, "Reliable and Economy Modes of Operation for Electric Vehicle-to-Home (V2H) System," 2018 5th IEEE Uttar Pradesh Section International Conference on Electrical, Electronics and Computer Engineering (UPCON), 2018, pp. 1-6, doi: 10.1109/UPCON.2018.8596932.
- [25] F. M. Shakeel and O. P. Malik, "Fuzzy Based Energy Management System for a Micro-grid with a V2G Parking Lot," 2020 IEEE Electric Power and Energy Conference (EPEC), 2020, pp. 1-5, doi: 10.1109/EPEC48502.2020.9320112.
- [26] J. Chen, Y. Zhang and W. Su, "An anonymous authentication scheme for plug-in electric vehicles joining to charging/discharging station in vehicle-to-Grid (V2G) networks," in China Communications, vol. 12, no. 3, pp. 9-19, Mar. 2015, doi: 10.1109/CC.2015.7084359.
- [27] J. Guo, J. Yang and P. Ivry, "Development of an Intelligent Control Platform for Vehicle-to-Grid Systems," 2020 9th International Conference on Renewable Energy Research and Application (ICRERA), 2020, pp. 83-87, doi: 10.1109/ICRERA49962.2020.9242685.
- [28] N. K. Bream, M. N. Joergensen, C. A. Knudsen, L. B. Kristensen and B. Yang, "A Charging Scheduling System for Electric Vehicles using Vehicle-to-Grid," 2019 20th IEEE International Conference on Mobile Data Management (MDM), 2019, pp. 351-352, doi: 10.1109/MDM.2019.00-36.
- [29] S. Das, P. Acharjee and A. Bhattacharya, "Charging Scheduling of Electric Vehicle incorporating Grid-to-Vehicle (G2V) and Vehicle-to-Grid (V2G) technology in Smart-Grid," 2020 IEEE International Conference on Power Electronics, Smart Grid and Renewable Energy (PESGRE2020), 2020, pp. 1-6, doi: 10.1109/PESGRE45664.2020.9070489.
- [30] M. Abul Masrur, Annette G, "Military-based Vehicle to Grid (V2G) and Vehicle to Vehicle (V2V) Microgrid - System Architecture and



- implementation" IEEE transaction on transportation Electrification PP(99(1-1), doi: 10.1109/TTE.2017.2779268.
- [31] D. Guo, P. Yi, C. Zhou and J. Wang, "Optimal electric vehicle scheduling in smart home with V2H/V2G regulation," 2015 IEEE Innovative Smart Grid Technologies - Asia (ISGT ASIA), 2015, pp. 1-6, doi: 10.1109/ISGT-Asia.2015.7387135.
- [32] A. Gautam, A. K. Verma and M. Srivastava, "A Novel Algorithm for Scheduling of Electric Vehicle Using Adaptive Load Forecasting with Vehicle-to-Grid Integration," 2019 8th International Conference on Power Systems (ICPS), 2019, pp. 1-6, doi: 10.1109/ICPS48983.2019.9067702.
- [33] M. Endo and K. Tanaka, "Evaluation of Storage Capacity of Electric Vehicles for Vehicle to Grid Considering Driver's Perspective," 2018 IEEE International Conference on Environment and Electrical Engineering and 2018 IEEE Industrial and Commercial Power Systems Europe (EEEIC / I&CPS Europe), 2018, pp. 1-5, doi: 10.1109/EEEIC.2018.8494218.



**Raghu Suraj Sundararajan** (member IEEE) was born on 27<sup>th</sup> September 1995 in Coimbatore, TamilNadu, India. Completed his B.Tech degree in mechatronics engineering from SRMIST, Chennai, TamilNadu, India by 2017.

He works as a teaching assistant and system designer at Memorial University of Newfoundland, St. John's, Canada, and Dotndash, respectively. Presently, he is a graduate student and doing a research based M. Eng in electrical engineering.

He has published conference papers on "Design of an IoT interface for a solar energy system with vehicle to home option for Newfoundland conditions" in IEEE IEMCON 2020, Canada, "Design of solar parking lot for 20 electric vehicles in St. John's, NL" in IEEE NECEC 2020, Canada and "Dynamic simulation of an Isolated Solar Powered Charging Facility for 20 Electric Vehicles in St. John's, Newfoundland" in IEEE NECEC 2020, Canada. Currently, his research focuses on the "Design of Vehicle to Grid energy system for Newfoundland conditions".



**M. Tariq Iqbal** received the B.Sc. (EE) degree from the University of Engineering and Technology, Lahore in 1986, the M.Sc. Nuclear Engineering degree from the Quaid-e-Azam University, Islamabad in 1988, and the Ph.D. degree in Electrical Engineering from the Imperial College London in 1994.

Since 2001 he is working at the Faculty of Engineering and Applied Science, Memorial University of Newfoundland. Presently he is full

Professor. His teaching activities cover a range electrical engineering topic, including renewable energy systems and power electronics. Currently, his research focuses on modeling and control of hybrid energy system.